

Article

Synthesis, Crystal Structure, and Nonlinear Optical Properties of a New Alkali and Alkaline Earth Metal Carbonate $\text{RbNa}_5\text{Ca}_5(\text{CO}_3)_8$

Qiaoling Chen ¹ and Min Luo ^{2,*}¹ School of Mathematics and Physics, Fujian University of Technology, Fuzhou 350118, China; cq1@fjut.edu.cn² Key Laboratory of Optoelectronic Materials Chemistry and Physics, Fujian Institute of Research on the Structure of Matter, Chinese Academy of Sciences, Fuzhou 350002, China

* Correspondence: lm8901@fjirsm.ac.cn; Tel.: +86-591-8375-0713

Academic Editors: Rukang Li, Shanpeng Wang, Qingfeng Yan and Helmut Cölfen

Received: 29 November 2016; Accepted: 28 December 2016; Published: 31 December 2016

Abstract: A new nonlinear optical (NLO) material, $\text{RbNa}_5\text{Ca}_5(\text{CO}_3)_8$, has been synthesized by the hydrothermal method. The crystal structure is established by single-crystal X-ray diffraction. $\text{RbNa}_5\text{Ca}_5(\text{CO}_3)_8$ crystallizes in the hexagonal crystal system with space group $P6_3mc$ (No. 186). The structure of $\text{RbNa}_5\text{Ca}_5(\text{CO}_3)_8$ can be described as the adjacent infinite $[\text{CaCO}_3]_\infty$ layers lying in the a-b plane bridged through standing-on-edge $[\text{CO}_3]$ groups by sharing O atoms (two-fold coordinated) to build a framework with four types of tunnels running through the b-axis. The Rb, Na, and $[\text{Na}_{0.67}\text{Ca}_{0.33}]$ atoms reside in these tunnels, respectively. The measurement of second harmonic generation (SHG) indicated that $\text{RbNa}_5\text{Ca}_5(\text{CO}_3)_8$ is a phase-matchable material, which had SHG responses of approximately $1 \times \text{KH}_2\text{PO}_4$ (KDP). Meanwhile, the results from the UV-VIS diffuse reflectance spectroscopy study of the powder samples indicated that the UV cut-off edges of $\text{RbNa}_5\text{Ca}_5(\text{CO}_3)_8$ is about 203 nm.

Keywords: carbonate; nonlinear optical crystal; UV; crystal growth

1. Introduction

UV nonlinear optical (NLO) crystals [1–8] have attracted widespread attention owing to their significant roles in laser science and related technology. Although several crystals with excellent nonlinear optical properties are well known, such as $\beta\text{-BaB}_2\text{O}_4$ [9], LiB_3O_5 [10] and CsB_3O_5 [11], and part of which have been commercially manufactured and used worldwide, the design and synthesis of new NLO materials with large macroscopic nonlinearities and wide transparency ranges are still a particularly difficult challenge.

According to the anionic group theory [12–14], the NLO coefficient of crystals mainly originate from a geometrical addition of the microscopic second-order susceptibility tensors of the anionic groups. The $[\text{BO}_3]^{3-}$ triangular groups with π -orbitals have been proven as favorite building units for designing NLO materials due to their abilities to produce a large microscopic second-order susceptibility and moderate birefringence. Numerous borates with the $[\text{BO}_3]^{3-}$ structural unit have been investigated [15–18]. Similarly, the same planar triangular $[\text{CO}_3]^{2-}$ groups are considered to be excellent NLO-active anionic groups as well. Recently, many excellent UV and deep-UV carbonate NLO crystals have been synthesized, such as ABCO_3F (A = K, Rb, Cs; B = Ca, Sr, Ba) [19], APbCO_3F (A = Rb, Cs) [20,21], $\text{K}_{2.70}\text{Pb}_{5.15}(\text{CO}_3)_5\text{F}_3$ [22], $\text{Na}_8\text{Lu}_2(\text{CO}_3)_6\text{F}_2$ [23], $\text{Na}_3\text{Lu}(\text{CO}_3)_2\text{F}_2$ [23], $\text{Na}_4\text{La}_2(\text{CO}_3)_5$ [24], $\text{CsNa}_5\text{Ca}_5(\text{CO}_3)_8$ [24], and $\text{Na}_3\text{Re}(\text{CO}_3)_3$ (Re=Y, Gd) [25]. Lately Lin's group confirmed that $[\text{CO}_3]^{2-}$ groups have a distinct advantage in birefringence and SHG effects in NLO crystals by theory calculation in comparison with $[\text{BO}_3]^{3-}$ group [26]. Thus, the $[\text{CO}_3]^{2-}$ ion was selected as a basic structural unit

to explore UV NLO materials. Additionally, it is well-known that the alkali metal and alkaline earth metal are ideal compositions in UV NLO materials because there are no electron transitions in the alkali metal-oxygen bond or alkaline earth metal-oxygen bond in the UV region [27,28]. Therefore, we expect that combining the $[\text{CO}_3]^{2-}$ groups with the alkali metal and alkaline earth metal will construct new kinds of UV NLO materials.

In the present work, the $\text{Na}_2\text{CO}_3\text{-RbCl-CaCl}_2$ systems were studied, attempting to synthesize new non-centrosymmetric alkali and alkaline earth metal carbonate crystals. As a result, we have successfully obtained a new acentric carbonate, $\text{RbNa}_5\text{Ca}_5(\text{CO}_3)_8$. It crystallizes in the hexagonal crystal system, space group $P6_3mc$ (No. 186), with $a = b = 10.075(3) \text{ \AA}$, $c = 12.639(5) \text{ \AA}$, $Z = 2$, $V = 1111.2(7) \text{ \AA}^3$. Herein its synthesis, crystal structure and some optical properties will be reported.

2. Results and Discussion

2.1. Crystal Structure Description

$\text{RbNa}_5\text{Ca}_5(\text{CO}_3)_8$ is isostructural to $\text{CsNa}_5\text{Ca}_5(\text{CO}_3)_8$ and crystallize into a hexagonal crystal system with a noncentrosymmetric space group of $P6_3mc$. The structure along the b-axis is shown in Figure 1. The structure can be described as the adjacent infinite $[\text{CaCO}_3]_\infty$ layers lying in the a-b plane bridged through the standing $[\text{CO}_3]$ groups by sharing O atoms (two-fold coordinated) to build a framework with four types of tunnels running through the b-axis. The Na, Rb, and $[\text{Na}_{0.67}\text{Ca}_{0.33}]$ atoms reside in these tunnels, respectively, where Na atoms are located in a seven-coordination environment with Na–O bond lengths ranging from 2.369(6) to 2.546(3) \AA , Rb atoms are located in an eight-coordination environment with Rb–O bond lengths ranging from 2.900(6) to 3.439(5) \AA and $[\text{Na}_{0.67}\text{Ca}_{0.33}]$ atoms are coordinated to nine O atoms with $\text{Na}_{0.67}\text{Ca}_{0.33}\text{-O}$ bond lengths ranging from 2.432(2) to 2.960(5) \AA . The C1, C2, and C4 atoms are coordinated to three O atoms to form planar $[\text{CO}_3]$ triangles with C–O bond lengths ranging from 1.232(4) to 1.295(1) \AA and O–C–O bond angles ranging from $114.6(1)^\circ$ to $122.7(7)^\circ$. However, C3 are surrounded by three O7 and one O6 to form a propeller-shape along c axis, which are caused by the split of O7. It is noteworthy that the $[\text{CO}_3]$ groups in two successive $[\text{CaCO}_3]_\infty$ layers present an opposite orientation (Figure 2a). According to anionic group theory, this arrangement of $[\text{CO}_3]$ groups makes almost no contribution to NLO susceptibilities. The macroscopic SHG effects, however, originated from the standing $[\text{CO}_3]$ group along c axis. It is regrettable that the standing-on-edge $[\text{C3O}_3]$ and $[\text{C4O}_3]$ groups are almost arranged oppositely to the c direction (see Figure 2b), which cancels the d_{33} contribution from $[\text{C4O}_3]$ group.

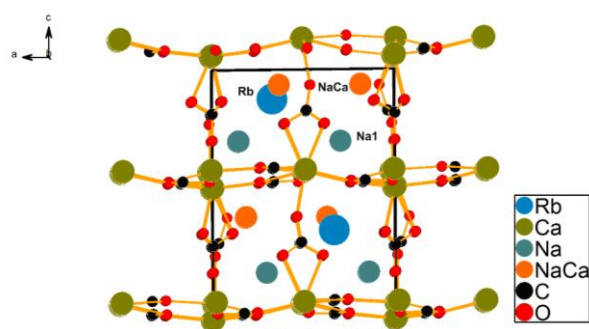


Figure 1. Crystal structure of $\text{RbNa}_5\text{Ca}_5(\text{CO}_3)_8$.

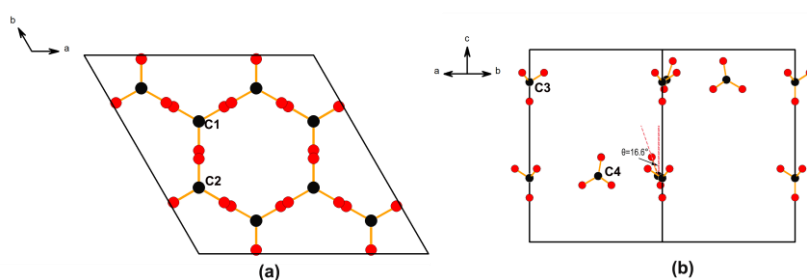
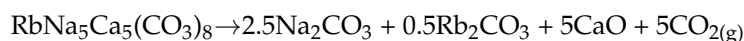


Figure 2. The arrangement of $[\text{CO}_3]^{2-}$ groups: (a) the flat-lying $[\text{CO}_3]^{2-}$ groups (b) the standing $[\text{CO}_3]^{2-}$ groups.

2.2. TG Analysis

The thermal behavior of $\text{RbNa}_5\text{Ca}_5(\text{CO}_3)_8$ is shown in Figure 3. As shown in Figure 3, $\text{RbNa}_5\text{Ca}_5(\text{CO}_3)_8$ is thermally stable up to about 600 °C. $\text{RbNa}_5\text{Ca}_5(\text{CO}_3)_8$ undergoes the weight loss between 600 °C and 850 °C due to the release of five moles of CO_2 (exp./th. = 25.03/24.97). The decomposition reaction is:



The reaction mechanism is confirmed by the residue PXRD. (See Figure S1 in the Supporting Information).

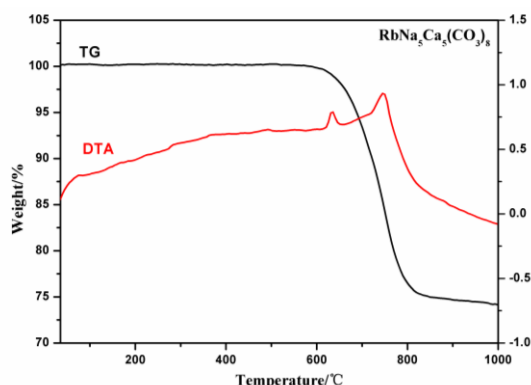


Figure 3. TG and DTA diagrams for $\text{RbNa}_5\text{Ca}_5(\text{CO}_3)_8$.

2.3. Diffuse-Reflectance Spectroscopy

As shown in Figure 4, UV-VIS diffuse reflectance spectra were collected for $\text{RbNa}_5\text{Ca}_5(\text{CO}_3)_8$ in the region of 200–2000 nm. Absorption (K/S) data were calculated from the following Kubelka-Munk function: $F(R) = (1-R)^2/2R = K/S$, where R is the reflectance, K is the absorption, and S is the scattering. In the (K/S)-versus- E plots, extrapolating the linear part of the rising curve to zero provided the onset of absorption. Optical diffuse reflectance spectrum studies indicated that the optical band gaps for $\text{RbNa}_5\text{Ca}_5(\text{CO}_3)_8$ was approximately 6.08 eV with UV cut-off edges of 203 nm.

2.4. NLO Properties

The curves of the SHG signal as a function of particle size from the measurements made on ground crystals of $\text{RbNa}_5\text{Ca}_5(\text{CO}_3)_8$ is shown in Figure 5. Based on the rule proposed by Kurtz and Perry, we can clearly see that the titled compound is phase-matching in the visible region. The KDP sample is used as a reference. The measurement of second-harmonic signal for $\text{RbNa}_5\text{Ca}_5(\text{CO}_3)_8$ is found to be about $1 \times \text{KDP}$.

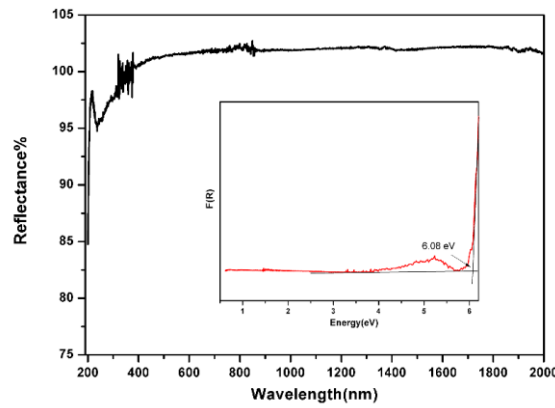


Figure 4. Diffuse reflectance curve of the powder sample of $\text{RbNa}_5\text{Ca}_5(\text{CO}_3)_8$.

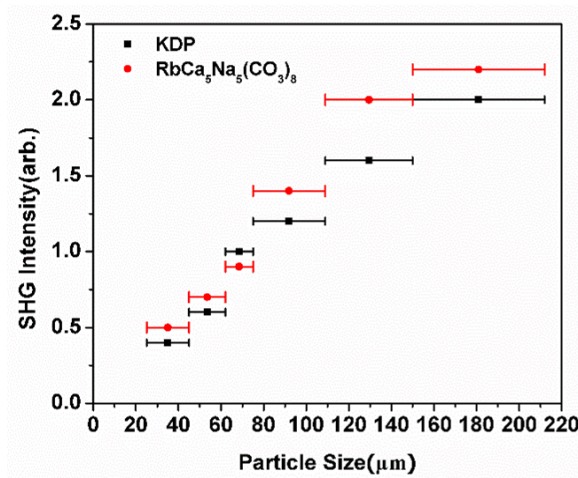


Figure 5. SHG measurements of $\text{RbNa}_5\text{Ca}_5(\text{CO}_3)_8$ ground crystals (red circle) with KDP (black square) as a reference.

2.5. Relationship between Structure and NLO Properties

According to the anionic group theory, the dipole transition from the cations to the anionic group ($[\text{CO}_3]$ in this case) is the off-site transition. Its value is about one order smaller than the dipole transition of the intra-atomic transitions within anionic groups. Thus, the main SHG coefficients have largely depended on the $[\text{CO}_3]$ anionic group. Therefore, based on the anionic group theory, the macroscopic second-order susceptibility $\chi^{(2)}$ may be expressed by Equation (1):

$$x_{ijk}^{(2)} = \frac{F}{V} \sum_P \sum_{i'j'k'} \alpha_{ii'} \alpha_{jj'} \alpha_{kk'} \beta_{i'j'k'}^{(2)}(P), \quad P = [\text{CO}_3] \quad (1)$$

where F is the correction factor of the localized field, V is the volume of the unit cell, $\alpha_{ii'}$, $\alpha_{jj'}$, and $\alpha_{kk'}$ are the direction cosines between the macroscopic coordinates axes of the crystal and the microscopic coordinates axes of $[\text{CO}_3]$ groups, and $\beta_{i'j'k'}$ is the microscopic second-order susceptibility tensors of an individual group. The $[\text{CO}_3]$ is a planar group in point group D_{3h} . Under the Kleinman approximation, there are only two non-vanishing second-order susceptibilities $\beta_{111}^{(2)} = -\beta_{122}^{(2)}$. The geometrical factor, g , can be derived from Equations (1) and (2) may be simplified according to the deduction process shown in ref [29]:

$$x_{ijk}^{(2)} = \frac{F}{V} \cdot g_{ijk} \cdot \beta_{111}^{(2)}([\text{CO}_3]) \quad (2)$$

In case of nonspontaneous polarization, the structural criterion C is defined as:

$$C = \frac{g}{n} \quad (3)$$

where n is the number of anionic groups in a unit cell.

Since the localized field (F) is dependent on the refractive index of crystal, for the convenience of discussion, we assume that the carbonates in our discussion have similar refractive index. Hence, from the Equations (2) and (3) we can see that the NLO coefficient $x_{ijk}^{(2)}$ is proportional to the density of the $[\text{CO}_3]$ group (n/V) and the structural criterion (C). According to the notation of Grice et al. [30], the $[\text{CO}_3]$ groups in $\text{RbNa}_5\text{Ca}_5(\text{CO}_3)_8$ had two arrangements, flat-lying and standing-on-edge. The flat-lying $[\text{CO}_3]$ groups in two successive $[\text{CaCO}_3]_\infty$ layers present an opposite orientation, which give almost no contribution to the C factor. The major contribution to the C factor is dependent on the standing-on-edge $[\text{CO}_3]$ groups along the c axis. It is worth noting that the standing-on-edge $[\text{CO}_3]$ groups exist as two sets of arrangements in the structure, among which two $[\text{CO}_3]$ groups are perfectly aligned along the c direction and the other six $[\text{CO}_3]$ groups skew towards the c axis by about 16.6° . However, it is regrettable that two sets of the arrangement present the opposite direction, which have negative contributions to the C factor. The accurately-calculated C factor for $\text{RbNa}_5\text{Ca}_5(\text{CO}_3)_8$ is 0.197. Although the density of the $[\text{CO}_3]$ group in title compound is moderate, the small C factor eventually results in the small macroscopic SHG effect.

In order to further illustrate how the macroscopic SHG responses affected by the arrangement of the NLO-active groups and the density of NLO-active groups, we compared $\text{RbNa}_5\text{Ca}_5(\text{CO}_3)_8$ with KSrCO_3F . In the KSrCO_3F , the $[\text{CO}_3]$ triangles are all exactly parallel to each other, giving a 100% optimum. Although the density of $[\text{CO}_3]$ groups in the $\text{RbNa}_5\text{Ca}_5(\text{CO}_3)_8$ (0.0144) is larger than that of KSrCO_3F (0.0089), the C value of $\text{RbNa}_5\text{Ca}_5(\text{CO}_3)_8$ is only 0.197, which results in the calculated value of $(n/V) \times C$ (\AA^{-3}) of $\text{RbNa}_5\text{Ca}_5(\text{CO}_3)_8$ (0.0028) is smaller than that of KSrCO_3F (0.0089). Therefore, the SHG value of $\text{RbNa}_5\text{Ca}_5(\text{CO}_3)_8$ is calculated to be 31.5% relative to KSrCO_3F . This result is approximately in accordance with the experimental value, which is 1/3, relative to KSrCO_3F for $\text{RbNa}_5\text{Ca}_5(\text{CO}_3)_8$. The calculation results were shown in Table 1 and the calculation results are in good agreement with the SHG measurements.

Table 1. NLO Effects of KSrCO_3F and $\text{RbNa}_5\text{Ca}_5(\text{CO}_3)_8$.

Crystals	SHG coefficient ($\times \text{KDP}$) ^a	Structural criterion C	densities of the $[\text{CO}_3]$ (n/V) (\AA^{-3})	$(n/V) \times C$ (\AA^{-3})
KSrCO_3F	3.33	1	0.0089	0.0089
$\text{RbNa}_5\text{Ca}_5(\text{CO}_3)_8$	1	0.197	0.0144	0.0028

3. Materials and Methods

3.1. Reagents

Na_2CO_3 (99.8%), CaCl_2 (99.8%), RbCl (99.8%) were purchased from Titan (Titan, Shanghai, China).

3.2. Synthesis and Crystal Growth

A mixture of Na_2CO_3 (2.12 g, 0.02 mol), CaCl_2 (0.444 g, 0.004 mol), RbCl (2.42 g, 0.02 mmol) and H_2O (10.0 mL) was sealed in an autoclave equipped with a Teflon liner (23 mL) and heated at 220°C for five days, followed by slow cooling to room temperature at a rate of $3^\circ\text{C}/\text{h}$. The reaction product was washed with deionized water and ethanol, and then dried in air. Colorless hexagonal prism-shaped $\text{RbNa}_5\text{Ca}_5(\text{CO}_3)_8$ crystals were obtained as a single phase in a yield of about 80% based on Ca.

3.3. Single-Crystal X-Ray Diffraction

Single-crystal X-ray diffraction data were collected at room temperature on a Rigaku Mercury CCD diffractometer (Rigaku, Tokyo, Japan) with graphite-monochromatic Mo K α radiation ($\lambda = 0.71073 \text{ \AA}$). A transparent block of crystal was mounted on a glass fiber with epoxy for structure determination. A hemisphere of data was collected using a narrow-frame method with ω -scan mode. The data were integrated using the CrystalClear program, and the intensities were corrected for Lorentz polarization, air absorption, and absorption attributable to the variation in the path length through the detector faceplate. Absorption corrections based on the multiscan technique were also applied. The structure of $\text{RbNa}_5\text{Ca}_5(\text{CO}_3)_8$ was solved by the direct methods using SHELXS-97 [31]. During the refinement for $\text{RbNa}_5\text{Ca}_5(\text{CO}_3)_8$, Na2 and Ca2 atoms were set to share the same sites, due to the large $U(\text{eq})$ and R values when these sites were assigned as Ca atoms. To retain charge balance, the occupancy ratios of Na/Ca were refined to be 0.67/0.33. Meanwhile, at this stage of refinement, the $U(\text{eq})$ of O(7) atom appeared to be very high. Consequently, the oxygen atom O(7) was split with a scale factor of 0.67. All thermal parameters were satisfying. Additionally, all non-hydrogen atoms were refined with anisotropic thermal parameters. The structure was verified using the ADDSYM algorithm from the program PLATON [32], and no higher symmetries were found. Relevant crystallographic data and details of the experimental conditions for $\text{RbNa}_5\text{Ca}_5(\text{CO}_3)_8$ are summarized in Table 2. (Database: CCDC 1510695, These data can be obtained free of charge via <http://www.ccdc.cam.ac.uk/conts/retrieving.html> (or from the CCDC, 12 Union Road, Cambridge CB2 1EZ, UK; Fax: +44 1223 336033; E-mail: deposit@ccdc.cam.ac.uk)) Atomic coordinates and isotropic displacement coefficients are listed in Table S1 and bond lengths in Table S2 in the Supporting Information.

Table 2. Crystal data and structure refinement for $\text{RbNa}_5\text{Ca}_5(\text{CO}_3)_8$.

Formula	$\text{RbNa}_5\text{Ca}_5(\text{CO}_3)_8$
Formula Mass(amu)	880.90
Crystal System	Hexagonal
Space Group	$P6_3mc$
a (Å)	10.075(3)
c (Å)	12.639(5)
A ($^\circ$)	90
γ ($^\circ$)	120
V (Å^3)	1111.2(7)
Z	2
$\rho(\text{calcd})$ (g/cm ³)	2.633
Temperature (K)	293(2)
λ (Å)	0.71073
F(000)	864
M (mm ⁻¹)	3.600
θ (deg)	2.33–27.50
Rint	0.0442
R/wR ($I > 2\sigma(I)$)	0.0409/0.1015
R/wR (all data)	0.0413/0.1018
GOF on F ²	1.117
Absolute Structure Parameter	0.00
Largest Diff. Peak and Hole (e/ Å^{-3})	1.069 and -0.835

$$R(F) = \frac{\sum ||F_o| - |F_c||}{\sum |F_o|}, wR(F_o^2) = [\sum w(F_o^2 - F_c^2)^2 / \sum w(F_o^2)^2]^{1/2}.$$

3.4. Powder X-Ray Diffraction

X-ray diffraction patterns of polycrystalline materials were obtained on a Rigaku Dmax2500 powder X-ray diffractometer (Rigaku, Tokyo, Japan) by using Cu K α radiation ($\lambda = 1.540598 \text{ \AA}$) at room temperature in the angular range of $2\theta = 5\text{--}65^\circ$ with a scan step width of 0.05° and a fixed time

of 0.2 s. The powder XRD pattern for the pure powder sample of $\text{RbNa}_5\text{Ca}_5(\text{CO}_3)_8$ shows a good agreement with the XRD pattern calculated from the single-crystal model (see Figure 6).

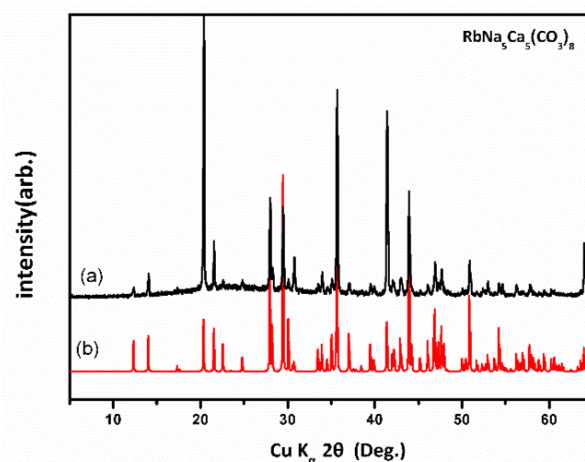


Figure 6. X-ray powder diffraction patterns of $\text{RbNa}_5\text{Ca}_5(\text{CO}_3)_8$.

3.5. Thermal Analysis

The TG/DTA scans were measured on a NETZSCH STA 449C (NETZSCH, Bavaria, Germany). Reference (Al_2O_3) and crystal samples (5–10 mg) were enclosed in Al_2O_3 crucibles and heated from room temperature to 1000 °C at a rate of 10 °C/min under a constant flow of nitrogen gas.

3.6. UV-VIS Diffuse Reflectance Spectroscopy

UV-VIS diffuse reflectance spectroscopy data were recorded at room temperature using a powder sample with BaSO_4 as a standard (100% reflectance) on a PerkinElmer Lambda-950 UV/VIS/NIR spectrophotometer and scanned at 200–2000 nm. Reflectance spectra were converted to absorbance using the Kubelka-Munk function [33,34].

3.7. Second-Harmonic Generation

Polycrystalline second-harmonic generation (SHG) signals were measured using the method adapted from Kurtz and Perry. Since SHG efficiencies are known to depend strongly on particle size, polycrystalline samples were ground and sieved into the following particle size ranges: 25–45, 45–62, 62–75, 75–109, 109–150, and 150–212 μm . The samples were pressed between glass microscope cover slides and secured with tape in 1-mm thick aluminum holders containing an 8-mm diameter hole. To make relevant comparisons with known SHG materials, crystalline KDP were also ground and sieved into the same particle size ranges. The samples were then placed in a light-tight box and irradiated with a pulsed laser. The measurements were performed with a Q-switched Nd:YAG laser at 1064 nm. A cutoff filter was used to limit background flash-lamp light on the sample, and an interference filter ($530 \pm 10\text{nm}$) was used to select the second harmonic for detection with a photomultiplier tube attached to a RIGOL DS1052E 50-MHz oscilloscope. This procedure was then repeated using the standard nonlinear optical materials KDP, and the ratio of the second-harmonic intensity outputs were calculated. No index-matching fluid was used in any of the experiment.

3.8. Scanning Electron Microscope (SEM)/Energy-Dispersive Analysis by X-Ray (EDX)

SEM/EDX analyses have been performed using a Hitachi S-3400N/Horiba Energy EX-250 instrument (Hitachi, Tokyo, Japan). EDX result reveals that the titled compound contain Rb, Na, and Ca with the ratio of 0.9:4.8:5.2.

4. Conclusions

In summary, $\text{RbNa}_5\text{Ca}_5(\text{CO}_3)_8$ with non-centrosymmetric structure, has been prepared under a subcritical hydrothermal condition. The results from the UV-VIS diffuse reflectance spectroscopy study of the powder sample indicated that the short-wavelength absorption edges of $\text{RbNa}_5\text{Ca}_5(\text{CO}_3)_8$ is about 203 nm. The SHG test shows that the compound exhibit SHG responses about one times KH_2PO_4 (KDP). Our future efforts will be devoted to growing large crystals of $\text{RbNa}_5\text{Ca}_5(\text{CO}_3)_8$ to further study their optical properties, such as refractive indices, the Sellmeier equations, second-order NLO coefficients, and laser damage threshold.

Supplementary Materials: The supplementary materials are available online at <http://www.mdpi.com/2073-4352/7/1/10/s1>.

Author Contributions: Qiaoling Chen conceived and designed this study, carried out experimental work (synthesis, crystallization and characterization) and wrote the manuscript. Min Luo conceived and coordinated the project.

Conflicts of Interest: The authors declare no conflict of interest.

References

1. Tran, T.T.; Yu, H.; Rondinelli, J.R.; Poeppelmeier, K.R.; Halasyamani, P.S. Deep Ultraviolet Nonlinear Optical Materials. *Chem. Mater.* **2016**, *28*, 5238–5258. [[CrossRef](#)]
2. Tran, T.T.; He, J.G.; Rondinelli, J.M.; Halasyamani, P.S. RbMgCO_3F : A New Beryllium-Free Deep-Ultraviolet Nonlinear Optical Material. *J. Am. Chem. Soc.* **2015**, *137*, 10504–10507. [[CrossRef](#)] [[PubMed](#)]
3. Xu, X.; Hu, C.L.; Kong, F.; Zhang, J.H.; Mao, J.G.; Sun, J. $\text{Cs}_2\text{GeB}_4\text{O}_9$: A new second-order nonlinear-optical crystal. *Inorg. Chem.* **2013**, *52*, 5831–5837. [[CrossRef](#)] [[PubMed](#)]
4. Wang, S.; Ye, N. Nonlinear optical crystal $\text{BiAlGa}_2(\text{BO}_3)_4$. *Solid State Sci.* **2007**, *9*, 713–717. [[CrossRef](#)]
5. Chen, J.; Luo, M.; Ye, N. Syntheses, characterization and nonlinear optical properties of sodium–scandium carbonate $\text{Na}_5\text{Sc}(\text{CO}_3)_4 \cdot 2\text{H}_2\text{O}$. *Solid State Sci.* **2014**, *36*, 24–28. [[CrossRef](#)]
6. Huang, L.; Zou, G.; Cai, H.; Wang, S.; Lin, C.; Ye, N. $\text{Sr}_2(\text{OH})_3\text{NO}_3$: the first nitrate as a deep UV nonlinear optical material with large SHG responses. *J. Mater. Chem. C* **2015**, *3*, 5268–5274. [[CrossRef](#)]
7. Ye, N.; Zeng, W.R.; Jiang, J.; Wu, B.C.; Chen, C.T.; Feng, B.H.; Zhang, X.L. New nonlinear optical crystal $\text{K}_2\text{Al}_2\text{B}_2\text{O}_7$. *J. Opt. Soc. Am. B* **2000**, *17*, 764–768. [[CrossRef](#)]
8. Sasaki, T.; Mori, Y.; Yoshimura, M.; Yap, Y.K.; Kamimura, T. Recent development of nonlinear optical borate crystals: key materials for generation of visible and UV light. *Mater. Sci. Eng. R Rep.* **2000**, *30*, 1–54. [[CrossRef](#)]
9. Chen, C.T.; Wu, B.C.; Jiang, A.D.; You, G.M. A new-type ultraviolet SHG crystal-Beta- BaB_2O_4 . *Sci. Sin. Ser. B* **1985**, *28*, 235–243.
10. Chen, C.; Wu, Y.; Jiang, A.; Wu, B.; You, G.; Li, R.; Lin, S. New nonlinear-optical crystal: LiB_3O_5 . *J. Opt. Soc. Am. B* **1989**, *6*, 616–621. [[CrossRef](#)]
11. Wu, Y.; Sasaki, T.; Nakai, S.; Yokotani, A.; Tang, H.; Chen, C. CsB_3O_5 : A new nonlinear optical crystal. *Appl. Phys. Lett.* **1993**, *62*, 2614. [[CrossRef](#)]
12. Chen, C.T.; Liu, G.Z. Recent Advances in Nonlinear Optical and Electro-Optical Materials. *Annu. Rev. Mater. Sci.* **1986**, *16*, 203–243. [[CrossRef](#)]
13. Chen, C.T.; Li, R.K. The Anionic Group Theory of The Non-Linear Optical Effect and Its Applications in the Development of New High-Quality NLO Crystals in the Borate Series. *Int. Rev. Phys. Chem.* **1989**, *8*, 65–91. [[CrossRef](#)]
14. Chen, C.T. Localized Quantal Theoretical Treatment, Based on an Anionic Coordination Polyhedron Model, for the Eo and Shg Effects in Crystals of the Mixed-Oxide Types. *Scientia Sinica* **1979**, *22*, 756–776.
15. Zou, G.; Zhang, L.; Ye, N. Synthesis, structure, and characterization of a new promising nonlinear optical crystal: $\text{Cd}_5(\text{BO}_3)_3\text{F}$. *CrystEngComm* **2013**, *15*, 2422. [[CrossRef](#)]
16. Yu, H.; Wu, H.; Pan, S.; Wang, Y.; Yang, Z.; Su, X. New salt-inclusion borate, $\text{Li}_3\text{Ca}_9(\text{BO}_3)_7 \cdot 2[\text{LiF}]$: A promising UV NLO material with the coplanar and high density BO_3 triangles. *Inorg. Chem.* **2013**, *52*, 5359–5365. [[CrossRef](#)] [[PubMed](#)]

17. Zhao, S.; Gong, P.; Bai, L.; Xu, X.; Zhang, S.; Sun, Z.; Lin, Z.; Hong, M.; Chen, C.; Luo, J. Beryllium-free $\text{Li}_4\text{Sr}(\text{BO}_3)_2$ for deep-ultraviolet nonlinear optical applications. *Nat. Commun.* **2014**, *5*, 4019. [[CrossRef](#)] [[PubMed](#)]
18. Xia, M.J.; Li, R.K. Structure and optical properties of a noncentrosymmetric borate $\text{RbSr}_4(\text{BO}_3)_3$. *J. Solid State Chem.* **2013**, *197*, 366–369. [[CrossRef](#)]
19. Zou, G.; Ye, N.; Huang, L.; Lin, X. Alkaline-alkaline earth fluoride carbonate crystals ABCO_3F (A = K, Rb, Cs; B = Ca, Sr, Ba) as nonlinear optical materials. *J. Am. Chem. Soc.* **2011**, *133*, 20001–20007. [[CrossRef](#)] [[PubMed](#)]
20. Tran, T.T.; Halasyamani, P.S.; Rondinelli, J.M. Role of Acentric Displacements on the Crystal Structure and Second-Harmonic Generating Properties of RbPbCO_3F and CsPbCO_3F . *Inorg. Chem.* **2014**, *53*, 6241–6251. [[CrossRef](#)] [[PubMed](#)]
21. Zou, G.; Huang, L.; Ye, N.; Lin, C.; Cheng, W.; Huang, H. CsPbCO_3F : a strong second-harmonic generation material derived from enhancement via p-pi interaction. *J. Am. Chem. Soc.* **2013**, *135*, 18560–18566. [[CrossRef](#)] [[PubMed](#)]
22. Tran, T.T.; Halasyamani, P.S. New fluoride carbonates: centrosymmetric $\text{KPb}_2(\text{CO}_3)_2\text{F}$ and noncentrosymmetric $\text{K}_{2.70}\text{Pb}_{5.15}(\text{CO}_3)_5\text{F}_3$. *Inorg. Chem.* **2013**, *52*, 2466–2473. [[CrossRef](#)] [[PubMed](#)]
23. Luo, M.; Ye, N.; Zou, G.; Lin, C.; Cheng, W. $\text{Na}_8\text{Lu}_2(\text{CO}_3)_6\text{F}_2$ and $\text{Na}_3\text{Lu}(\text{CO}_3)_2\text{F}_2$: Rare Earth Fluoride Carbonates as Deep-UV Nonlinear Optical Materials. *Chem. Mater.* **2013**, *25*, 3147–3153. [[CrossRef](#)]
24. Luo, M.; Wang, G.; Lin, C.; Ye, N.; Zhou, Y.; Cheng, W. $\text{Na}_4\text{La}_2(\text{CO}_3)_5$ and $\text{CsNa}_5\text{Ca}_5(\text{CO}_3)_8$: Two new carbonates as UV nonlinear optical materials. *Inorg. Chem.* **2014**, *53*, 8098–8104. [[CrossRef](#)] [[PubMed](#)]
25. Luo, M.; Lin, C.; Zou, G.; Ye, N.; Cheng, W. Sodium–rare earth carbonates with shorite structure and large second harmonic generation response. *CrystEngComm* **2014**, *16*, 4414–4421. [[CrossRef](#)]
26. Kang, L.; Luo, S.Y.; Huang, H.W.; Ye, N.; Lin, Z.S.; Qin, J.G.; Chen, C.T. Prospects for Fluoride Carbonate Nonlinear Optical Crystals in the UV and Deep-UV Regions. *J. Phys. Chem. C* **2013**, *117*, 25684–25692. [[CrossRef](#)]
27. Yang, Y.; Pan, S.L.; Hou, X.L.; Wang, C.Y.; Poepplmeier, K.R.; Chen, Z.H.; Wu, H.P.; Zhou, Z.X. A congruently melting and deep UV nonlinear optical material: $\text{Li}_3\text{Cs}_2\text{B}_5\text{O}_{10}$. *J. Mater. Chem.* **2011**, *21*, 2890–2894. [[CrossRef](#)]
28. Wang, S.; Ye, N.; Li, W.; Zhao, D. Alkaline beryllium borate NaBeB_3O_6 and $\text{ABe}_2\text{B}_3\text{O}_7$ (A = K, Rb) as UV nonlinear optical crystals. *J. Am. Chem. Soc.* **2010**, *132*, 8779–8786. [[CrossRef](#)] [[PubMed](#)]
29. Ye, N.; Chen, Q.X.; Wu, B.C.; Chen, C.T. Searching for new nonlinear optical materials on the basis of the anionic group theory. *J. Appl. Phys.* **1998**, *84*, 555–558. [[CrossRef](#)]
30. Grice, J.D.; Maisonneuve, V.; Leblanc, M. Natural and Synthetic Fluoride Carbonates. *Chem. Rev.* **2006**, *107*, 114–132. [[CrossRef](#)] [[PubMed](#)]
31. Sheldrick, G.M. A short history of SHELX. *Acta Crystallogr. Sect. A* **2008**, *64*, 112–122. [[CrossRef](#)] [[PubMed](#)]
32. Spek, A.L. Single-crystal structure validation with the program PLATON. *J. Appl. Crystallogr.* **2003**, *36*, 7–13. [[CrossRef](#)]
33. Tauc, J. UV-VIS. *Mater. Res. Bull.* **1970**, *5*, 721–730. [[CrossRef](#)]
34. Kubelka, P.; Munk, F.Z. Ein Beitrag zur Optik der Farbanstriche. *Tech. Phys.* **1931**, *12*, 593–601. (In German)



© 2016 by the authors; licensee MDPI, Basel, Switzerland. This article is an open access article distributed under the terms and conditions of the Creative Commons Attribution (CC-BY) license (<http://creativecommons.org/licenses/by/4.0/>).